



Fermi National Accelerator Laboratory

FERMILAB-PUB-92/193-T
TMUP-HEL-9205
KEK-TH-337
KEK Preprint 92-55

Neutrino Flavor Mixing, Spin Precession and the Solar Neutrino Experiments

Hiroshi Nunokawa ^{1,2} and Hisakazu Minakata ^{1,3}

¹ *Department of Physics, Tokyo Metropolitan University
1-1 Minami-Osawa, Hachioji, Tokyo 192-03, Japan*

² *Physics Department, National Laboratory for High Energy Physics
(KEK), 1-1 Oho, Tukuba, Ibaraki 305, Japan*

³ *Theory Group, Fermilab, P.O. Box 500, Batavia, Illinois 60510, U.S.A.*

Abstract

The predictions of the hybrid solution of the solar neutrino problem which combines resonant flavor mixing and spin precession are confronted with the ³⁷Cl, the Kamiokande II, and the ⁷¹Ga experiments. In addition to the two known solutions we find a new parameter region which is consistent with the experiments and is characteristic to the hybrid mechanism. We emphasize the importance of measuring ⁷Be neutrinos to distinguish these three solutions.



The solar neutrino problem [1], the deficit of solar neutrinos compared with that predicted by the standard solar model, has been lasted for more than 20 years since the beginning of the Davis ^{37}Cl experiment [2]. Now the three types of experiments are in array to observe solar neutrinos which detect their different parts of the energy spectra. The Kamiokande II experiment [3], which detects neutrinos through Cherenkov light of recoil electrons, can tell us from which directions neutrinos came and presented the first direct evidence for the nuclear fusion reaction by which the sun shines.

Two experiments which use ^{71}Ga as target nucleus began to operate more recently. The Soviet America Gallium Experiment (SAGE) [4] has been taken their data since 1989 and recently the GALLEX group [5] presented their data after about one-year operation since May 1991. These ^{71}Ga experiments are believed to provide us the crucial data by which we can decide whether the solar neutrino problem is the issue of the solar physics or that of the particle physics.

In this Letter we address the implication of the results of these three types of solar neutrino experiments to particles physics. At present the statistics of the ^{71}Ga experiments are not good enough to verify that the particle physics is relevant for the solar neutrino problem. Nevertheless, there is a good reason to suspect that it is, given the fact that the results of the all existing experiments [2-5] give the values less than or equal to ~60% of the standard solar model.

One of the charming solution of the solar neutrino problem is the Mikheyev-Smirnov-Wolfenstein (MSW) mechanism [6] for the resonant enhancement of the neutrino flavor conversion in the solar matter. The GALLEX Group [5] presented the result of their analysis and concluded

that the two small regions on the $\Delta m^2 - \sin^2 2\theta$ parameter plane can be selected out by requiring the 90% level consistency between the ^{37}Cl , the Kamiokande II, and the GALLEX results. Here Δm^2 and θ indicate, respectively, the neutrino mass-squared difference and the vacuum mixing angle between electron and a heavier flavor neutrinos.

The other interesting proposal for the solution of the solar neutrino deficit is the resonant enhancement of the neutrino spin-flavor precession [7] tied up with the possibility of strong magnetic fields extended over the interior of the sun. This proposal was motivated by an intriguing suggestion [8] that the event rate of the ^{37}Cl experiment might be in anticorrelation with the sunspot activity. It was followed by an interesting idea [9] that it may be due to a large neutrino magnetic moment but this possibility has encountered the difficulty of the matter-effect suppression. It then revived by the proposal of the resonant spin-flavor precession mechanism with transition magnetic moments. The unanswered problem in this proposal is that, given the various astrophysical bounds [10] on the magnetic moment of neutrinos, $\mu < 10^{-11} \mu_B$ with μ_B being the Bohr magneton, it requires, as order of magnitude, 10 kG solar magnetic field which may or may not exist in the sun. Nevertheless, assuming that the anticorrelation is real, there would be no explanations beyond this proposal.

In this Letter we wish to present a part of the results of our extensive analysis of the hybrid mechanism which combines the flavor-MSW and the spin-flavor precession. Since the flavor-MSW is built-in in our mechanism we have two parameter regions, similar to that of pure flavor-MSW case, consistent with the experiments. (See later for more detail.) In addition to these solutions we do find a new (third) parameter region which is

characteristic to the hybrid mechanism. Then we also discuss the way how we can distinguish these three parameter regions in terms of the ongoing or the planned solar neutrino experiments.

In the present analysis we confine ourselves to the constraints on the parameter region imposed by the over-all reduction rates of the solar neutrino flux measured by these three-types of experiments. The reason why we do not enter into the detailed structure of the time variation is three-fold: (1) It is difficult, at least at present, to determine the structure of the anti-correlation since its statistical significance is limited in the ^{37}Cl [11] and also in the Kamiokande II data [12]. (2) To properly address the time variation we have to deal with the problem of the uncertainty of the toroidal magnetic fields in the sun. Not only their absolute value but also their radial dependence are poorly known. (3) Once proposed, the hybrid mechanism can be used as a model of generating reduced and barely time-dependent flux by an appropriate choice of parameters. In short, the analysis of the present Letter is meant to impose mild constraints on the parameters of the hybrid mechanism and also to provide ways to further distinguish selected parameter regions.

As a particular version of the spin-flavor precession mechanism we work with the case of two flavor (e and μ) Majorana neutrinos. The reasons for working with Majorana neutrinos are: (1) The transition magnetic moment is natural for Majorana neutrinos (if any). (2) The supernova constraint is milder for Majorana neutrinos because their right-handed pieces are not sterile.

Now let us start by writing down the Schrodinger-like equation which describes the neutrino propagation in the sun. We denote the four

component neutrino wave function as $\Psi^T=(\nu_e,\nu_\mu,\bar{\nu}_e,\bar{\nu}_\mu)$ The time evolution of Ψ is governed by the equation $i\frac{d}{dt}\Psi=H\Psi$ with the Hamiltonian matrix

$$H = \begin{bmatrix} A_+ & M \\ -M & A_- \end{bmatrix}, \quad (1)$$

with

$$A_\pm = \begin{bmatrix} \pm a_{\nu e}(r) + \frac{\Delta m^2}{4E} \sin^2 \theta & \frac{\Delta m^2}{4E} \sin 2\theta \\ \frac{\Delta m^2}{4E} \sin 2\theta & \pm a_{\nu \mu}(r) + \frac{\Delta m^2}{4E} \cos^2 \theta \end{bmatrix}$$

and

$$M = \begin{bmatrix} 0 & \mu B \\ -\mu B & 0 \end{bmatrix}.$$

In Eq. (1) E implies the neutrino energy, $a_{\nu e}$ and $a_{\nu \mu}$ represent the change of the index of refraction due to the scattering with charge-neutral matter:

$$a_{\nu e}(r) = \sqrt{2}G_F(N_e - \frac{1}{2}N_n),$$

$$a_{\nu \mu}(r) = -(G_F/\sqrt{2})N_n,$$

where N_e and N_n denotes, respectively, the electron and the neutron number densities in the sun.

We numerically integrate the Schrodinger equation to simulate the neutrino evolution in the sun. We use the standard-solar-model calculation of Bahcall and Ulrich [13] as input and discuss the reduction rate by referring this particular calculation. Our numerical code includes all neutrino sources which contribute to the ^{37}Cl , the Kamiokande II, and the ^{71}Ga experiments, respectively. We perform a complete integral over the neutrino energy spectra with appropriate cross sections and the detection efficiency. On the other hand we do not carry out the sum over production points by assuming that they are produced at the center of the sun. Instead of elaborating this point we restrict ourselves to the region of Δm^2 where the resonances takes place in outer region than that of the neutrino production so that our approximation makes sense. It roughly corresponds to $\Delta m^2 < 5 \times 10^{-5} \text{ eV}^2$ for ^8B neutrinos and to $\Delta m^2 < 10^{-6} \text{ eV}^2$ for pp neutrinos.

There exist large uncertainties in the magnetic fields in the solar interior. We simply assume the toroidal magnetic field with constant strength throughout the sun. As we emphasized before it may not be enough to work with this simple choice when we attempt to make a detailed analysis of the time variation. But it may be a meaningful approximation for our present purpose. The moral here is that we restrict ourselves to the parameter region where the spin-flavor resonance occurs at the convective layer of the sun. This is because we do not know for sure if the strong magnetic field exists in the radiation zone and if it is correlated with the solar activity. This requirement roughly implies that $\Delta m^2 < 5 \times 10^{-6} \text{ eV}^2$ for ^8B neutrinos and $\Delta m^2 < 2 \times 10^{-7} \text{ eV}^2$ for pp neutrinos.

In this Letter we only present the results with magnetic field strength $\mu B = 2 \times 10^{-10} \mu_B \text{kG}$. But we also make brief remarks on how the results change when the magnetic field strength is varied. Since the energy scale $10^{-10} \mu_B \text{kG}$ is a natural scale for the physics related with the magnetic field in the sun we shall call it as 1 Solar Zeeman Unit (SZU), hereafter, for simplicity of our notation. In fact it is roughly equal to the inverse thickness of the convection zone.

In Fig.1 we present the result of our computation with $\mu B = 2$ SZU by drawing regions of parameters consistent with the ^{37}Cl (dashed line) and the Kamiokande II (dotted line) experiments at 2σ level. The shaded region implies the overlapping region of these two regions. In regions of Δm^2 greater than $2 \times 10^{-7} \text{eV}^2$ the shape of the contours resembles that of the pure flavor-MSW mechanism. As we emphasized before [14] it is one of the nice features of the hybrid mechanism, that is, the spin-flavor resonance naturally occurs just in the convective layers of the sun for not so strong magnetic fields.

In Fig.1 we also depict the iso-SNU contour for the ^{71}Ga experiment. If we believe in the GALLEX result, $83 \pm 19 \pm 8$ SNU, at 2σ level (41-125 SNU) then we are left with three disconnected regions of parameter space. Namely, we obtain a new consistent parameter region around $\Delta m^2 = 7 \times 10^{-8} \text{eV}^2$ and $\sin^2 2\theta = 0.02$, in addition to the two flavor-MSW dominated solution. If we take the SAGE result [4], $20 \pm 15_{20 \pm 32}$ SNU, then whole obelique branch of the shaded region is consistent with these three experiments. Since the SAGE result is consistent with that of GALLEX and since the latter is more restrictive than the former we will concentrate ourselves on the GALLEX result in the following part of this

Letter. A short comment on errors; We have combined the statistical and the systematic errors of the Kamiokande II and the GALLEX experiments by treating them as gaussian errors.

A brief remark on the magnetic field dependence; With $\mu B = 3$ SZU magnetic field our new solution moves to a smaller Δm^2 region and becomes an almost pure spin precession solution. That is, the region extends to the one which can be approximated as $2 \times 10^{-8} \text{ eV}^2 < \Delta m^2 < 3 \times 10^{-8} \text{ eV}^2$ and $\sin^2 2\theta < 0.06$

Now let us enter into the problem how we can distinguish among the three regions of consistent solution. We first examine the possibility of doing it by accurately measuring the energy spectrum in the Super-Kamiokande detector. We arbitrarily pick up three points (a)-(c) as representatives of these three solutions: (a) $\Delta m^2 = 6 \times 10^{-6} \text{ eV}^2$, $\sin^2 2\theta = 0.01$; (b) $\Delta m^2 = 2 \times 10^{-5} \text{ eV}^2$, $\sin^2 2\theta = 0.7$; (c) $\Delta m^2 = 7 \times 10^{-8} \text{ eV}^2$, $\sin^2 2\theta = 0.02$. Notice that the solution (c) is the new one with magnetic field strength $\mu B = 2$ SZU. Since the solutions (a) and (b) is flavor-MSW dominated we shall switch off the magnetic field in discussing the solutions (a) and (b) from here on. Therefore, (a) and (b) is the pure flavor-MSW solutions and (c) is the hybrid solution with 2 SZU magnetic field.

In Fig.2 we present (i) the way how ^8B neutrino spectrum is distorted, and (ii) what the energy spectra of recoil electrons look like, for these three set of parameters. They are compared with that of the expectation by the standard solar model. We have fine-tuned the parameters of (a), (b), and (c) so that they yield approximately equal numbers of events. In Fig.2-(iii) we depict the ratio of the recoil electron spectra to that of the standard solar model. According to Ref. [15] the error bars expected for three-years operation of the Super-Kamiokande is about ± 0.02 to ± 0.03 at electron

energies around 12 MeV. Therefore, the discrimination among these three solutions only by measuring the shape of the electron energy spectrum will require operation of the high-statistics water Cherenkov detector over many years [16].

Let us look for another possibility of discriminating these three solutions. In Fig.3 we plot the survival probabilities of electron neutrinos when they reach to a detector. From this figure it is obviously important to detect low energy, 0.5-6 MeV, neutrinos. One of the most interesting source of low energy neutrinos is from ${}^7\text{Be}$. It consists of two lines at 0.862 MeV and 0.384 MeV with branching ratios of 90% and 10%, respectively. We note that there are at least two planned experiments which are suitable for this purpose; one is the BOREXINO [17] and the other is the Indium-loaded liquid scintillation detector [18].

We emphasize again the importance of measuring low energy neutrinos to distinguish the two flavor-MSW solutions even if one disbelieves in the strong magnetic fields in the sun.

If we only want to discriminate our hybrid solutions around the parameter (c) from that of the flavor-MSW's then there may be an another way of doing the job. In Fig.4 we plot the composition of the four components of neutrinos and their contributions to the electron energy spectrum in water Cherenkov detectors at the parameters (c). We observe that the neutrino deficit is mostly due to the spin-flavor precession as indicated by the large $\bar{\nu}_\mu$ component in Fig.4-(i). Nonetheless, it does not yield large contribution to the electron energy spectrum because their cross section is factor of 7 smaller compared to that of electron neutrinos, as one can see in Fig.4-(ii). The fact that our new solution is mostly due to the

spin-flavor precession allows us another prediction: If the magnetic field in the convective layer of the sun is not time-independent one should detect it via the time variation of the count rate at the Super-Kamiokande, a high statistics water-Cherenkov detector.

On the other hand we do not expect time variation of the ^{71}Ga count rate as one may observe in Fig.1. (Our new solution acts like the flavor-MSW for the ^{71}Ga experiment as indicated in the figure.) Our last comment is that if one could measure and separate the neutral current reactions very accurately, then it would be possible to discriminate our new solution to the flavor-MSW's. To carry it out one must detect $\sim 20\%$ difference between $\nu_{\mu}e$ and $\bar{\nu}_{\mu}e$ cross sections.

One of the authors (H.N.) expresses his gratitude to Makoto Kobayashi for allowing him to visit KEK. The other (H.M.) thanks Wick Haxton for useful conversations and Bill Bardeen for warm hospitality extended to him at Fermilab where this work is completed.

References and Footnotes

- [1] J. N. Bacall, *Neutrino Astrophysics* (Cambridge University Press, New York, 1989).
- [2] B. Cleveland et al., in *Proceedings of the 25th International Conference on High Energy Physics*, Vol. I, page 667, edited by K. K. Phua and Y. Yamaguchi (World Scientific, Singapore, 1991).
- [3] K.S. Hirata et al., *Phys. Rev. D*44, 2241 (1991).
- [4] A.I. Abazov et al., *Phys. Rev. Lett.* 67, 3332 (1991).
- [5] P. Anselmann et al., (GALLEX collaboration), Reports GX1 and GX2, 1992.
- [6] S.P. Mikheyev and A. Smirnov, *Nuovo Cimento* 9C, 17 (1986) ; L. Wolfenstein, *Phy. Rev. D*17, 2369 (1978).
- [7] C.S. Lim and W.J. Marciano, *Phys. Rev. D*37, 1368 (1988); E. Kh. Akhmedov, *Phys. Lett.* B213, 64 (1988); H. Minakata and H. Nunokawa, *Phys. Rev. Lett.* 63, 121 (1989).
- [8] R. Davis, Jr., in *Proceedings of the Seventh Workshop on Grand Unification*, Toyoma, Japan 1986, edited by J. Arafune (World Scientific Singapore, 1987).
- [9] M.B. Voloshin, M.I. Vysotsky, and L.B. Okun, *Yad. Fiz.* 44, 677 (1986) [*Sov. J. Nucl. Phys.* 44, 440 (1986)].
- [10] M. Fukugita and S. Yazaki, *Phys. Rev. D*36 , 3817 (1987); G. Raffelt, *Astrophys. J.* 365 , 559 (1990) R. Barbieri and R.N. Mohapatra, *Phys. Rev. Lett.* 61, 27 (1988); J.M. Lattimer and J. Cooperstein, *ibid.* 61, 23 (1988) ; D. Notzold, *Phys. Rev. D*38, 1658 (1988).
- [11] H. Nunokawa and H. Minakata, *Int. J. Mod. Phys. A*6, 2347 (1991); B. W. Filippone and P. Vogel, *Phys. Lett.* B246, 546 (1990); G.

Fiorentini and G. Mezzorani, *ibid.* B253, 181 (1991). For a somewhat different conclusion, see J. N. Bahcall and W. H. Press, *Astrophys. J.* 370, 730 (1991).

- [12] In spite of the general belief that the Kamiokande II result implies no time variation their data [3], in particular with equal (9.3 MeV) detection threshold over all period, slightly favors the time variation in anticorrelation with solar activity over a constant flux. It will be discussed in H. Nunokawa, Dr. of Science thesis (in preparation).
- [13] J.N. Bahcall and R.K. Ulrich, *Rev. Mod. Phys.* 60, 297 (1988).
- [14] H. Minakata and H. Nunokawa in Ref. [7].
- [15] Y. Totsuka, Talk presented at the International Symposium on Underground Physics Experiments, at Science Council of Japan, April 1990, Institute for Cosmic-Ray Research Report -227-90-20.
- [16] Our calculation does not take into account the energy resolution of the detector. The situation would become worse if it is done.
- [17] The BOREXINO detector is the prototype for the B solar neutrino detector BOREX proposed by R.S. Raghavan and S. Pakvasa, *Phys. Rev. D* 37, 849 (1988).
- [18] Y. Suzuki et al., *Nucl. Instrm. Methods.* A293, 615 (1990); K. Inoue et al., Talk presented at the Fourth Workshop on Elementary-Particle Picture of the Universe, Izu, November 1990, Institute for Cosmic-Ray Research Report -252-91-21.

Figure Captions

- Fig.1 The parameter regions consistent with the ^{37}Cl (dashed line) and the Kamiokande II (dotted line) experiments at 2σ level are drawn on $\Delta m^2 - \sin^2 2\theta$ parameter plane for the magnetic field strength of $\mu\text{B} = 2 \text{ SZU} = 2 \times 10^{-10} \mu_{\text{B}} \text{ kG}$. The shaded region indicates the consistent parameter regions with both experiments. Also plotted as iso-SNU contours (solid line) are the expected yields at the ^{71}Ga detectors.
- Fig.2 Presented are (i) the way how ^8B neutrino spectrum is distorted, (ii) the energy spectra of recoil electrons compared with that of the expectation by the standard solar model (indicated by solid line), (iii) the ratio of the recoil electron spectra to that of the standard solar model, for the three set of parameters (a, indicated by dotted line), (b, dashed line), and (c, dash-dotted line) described in the text. In (i) and (ii) the spectra are normalized so that the standard-solar-model values integrate to unity.
- Fig.3 The survival probabilities of electron neutrinos are plotted as a function of the neutrino energy for the three set of parameters (a), (b), and (c) with same line symbols as in Fig.2.
- Fig.4 Plotted are (i) the composition of the four components of neutrinos and (ii) their contributions to the electron energy spectrum in water-Cherenkov detectors at the parameters (c). The thin-solid line indicate the expectation of the standard solar model. The bold-solid, dashed, dotted, and the dash-dotted lines in (ii) are for $\nu_e, \nu_\mu, \bar{\nu}_\mu$, and the total, respectively.

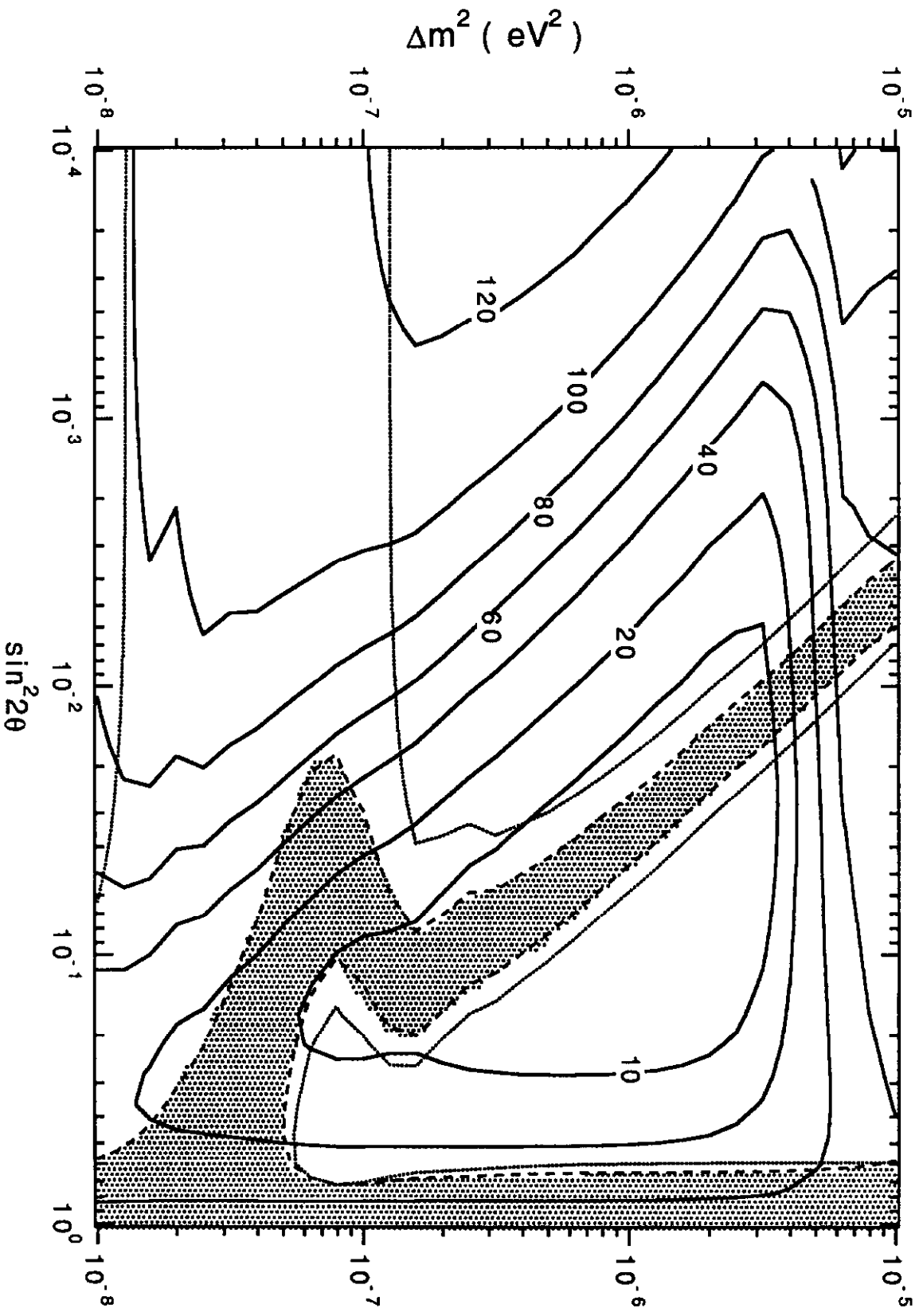


Fig. 1

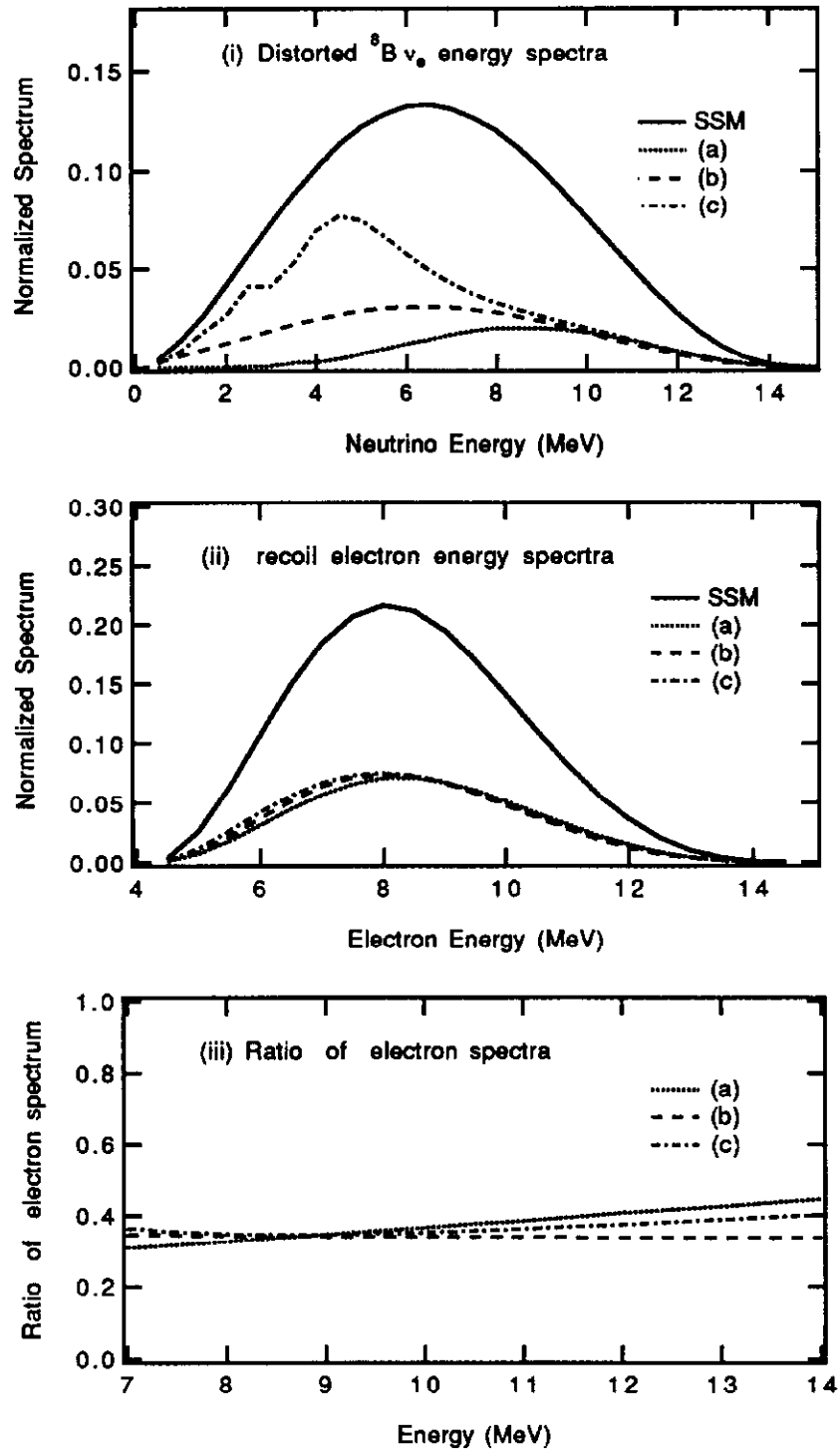


Fig. 2

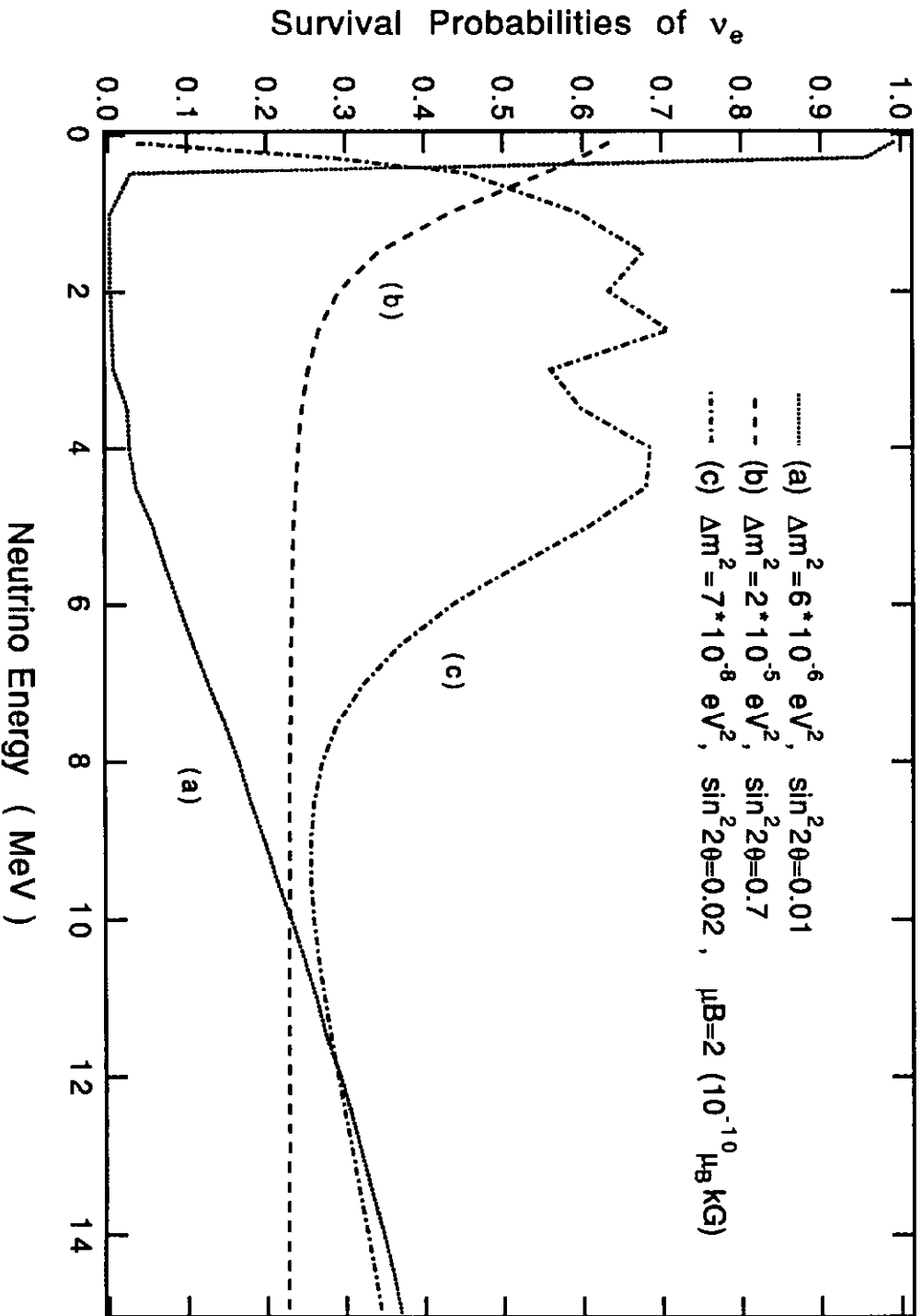


Fig. 3

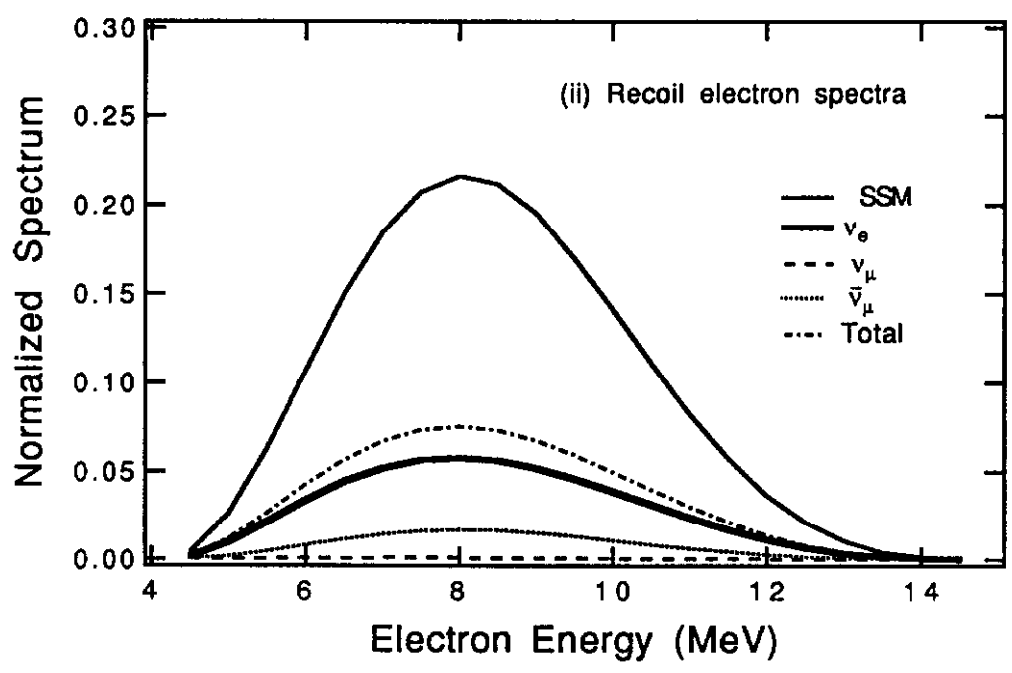
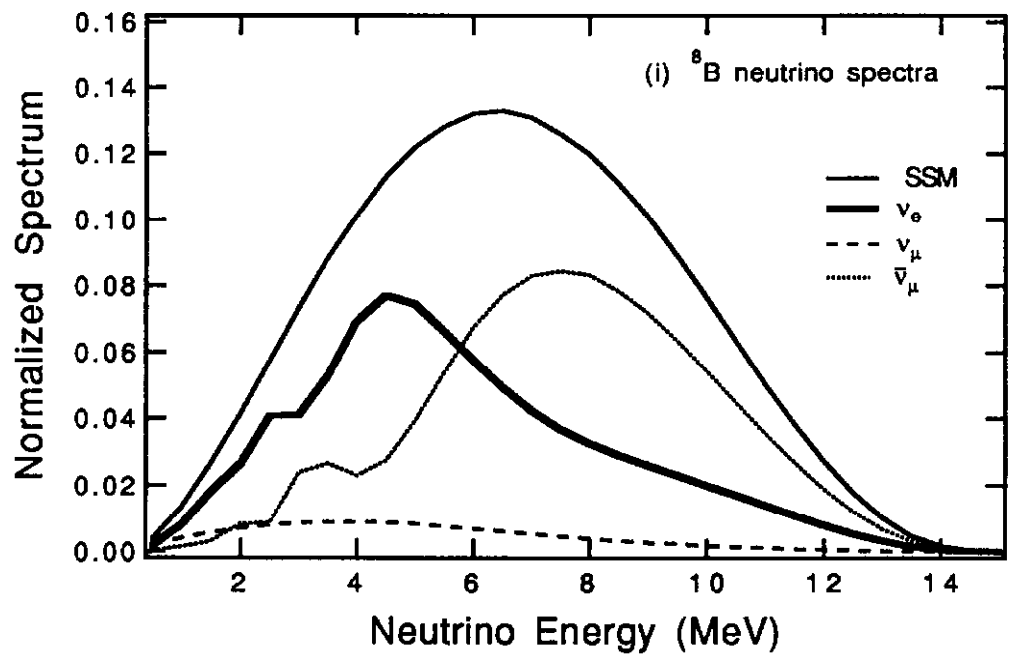


Fig. 4